The extra-terminal domain drives the role of BET proteins in transcription

Iwona Pasionek[1,†], John B. Ridenour[1,†], Agnieszka Machowska[1,†], Magdalena Donczew[1], Michael T. Kinter[2], Kevin A. Boyd[1], Rafal Donczew[1,3,*]

[1] Cell Cycle and Cancer Biology Research Program, Oklahoma Medical Research Foundation, Oklahoma City, OK, 73104, USA.
[2] Aging and Metabolism Research Program, Oklahoma Medical Research Foundation, Oklahoma City, OK, 73104, USA.
[3] Department of Cell Biology, University of Oklahoma Health Sciences Center, Oklahoma City, OK, 73104, USA.
[†] These authors contributed equally to this work.
[*] To whom correspondence should be addressed. Tel: 405-271-7437; Email: rafal-donczew@omrf.org.

Abstract

BET proteins facilitate the transcription of most eukaryotic genes, yet the specific mechanisms underlying their function remain incompletely understood. As chromatin readers, BET proteins use tandem bromodomains to recognize acetylated lysine residues on histones and other protein partners. However, recent evidence indicates that bromodomain activity alone does not account for the full spectrum of BET protein functions, underscoring the importance of additional conserved domains. Here, we systematically evaluated all conserved domains of BET proteins and identified the extra-terminal (ET) domain as essential for cell viability, genome-wide transcription, and BET chromatin occupancy. Moreover, we demonstrate that the ET domain exerts these effects by acting as a central hub for interactions with multiple transcriptional regulators. Our findings advance the current understanding of BET protein biology and reveal potential mechanisms by which cells can evade bromodomain inhibition under pathological conditions.

Introduction

Bromodomains (BDs) are reader modules that recognize acetylated lysine residues on histones and other protein targets[1]. Members of the bromodomain and extra-terminal domain (BET) family are conserved chromatin readers that play central roles in transcription regulation[2–5]. Consistent with this function, BET proteins have been implicated in sustaining pathological transcriptional programs across various human diseases[6,7]. Pharmacological inhibition of BET bromodomains represents a promising therapeutic strategy for cancer and other disorders; however, resistance to BD inhibitors frequently emerges, highlighting the need for alternative approaches to target BET proteins[8–12]. However, a comprehensive model describing how BET proteins regulate transcription remains elusive.

All three mammalian BET proteins expressed in somatic tissues (BRD2, BRD3, and BRD4) contribute to gene transcription, but BRD4 functions as the dominant BET factor, with primary roles in transcription elongation[3–5,13,14]. Budding yeast encode two BET proteins (Bdf1 and Bdf2, referred to here as Bdf1/2), at least one of which is required for viability. Bdf1/2 make overlapping contributions to transcription; however, similar to BRD4 in mammalian cells, yeast cells rely predominantly on Bdf1[2,15]. Mechanistically, Bdf1/2 support both the initiation and elongation phases of transcription[2]. Notably, mammalian BET proteins have also been

implicated in transcription initiation, indicating that BET-dependent transcriptional functions are broadly conserved across eukaryotic lineages[4,14,16].

According to the canonical model, the tandem BDs serve as the primary module supporting BET protein function[1,8,17]. The multiply acetylated N-terminal tail of histone H4 is a preferred target of most BET BDs, including both BDs of Bdf1[14,18,19]. However, we previously showed that rapid depletion of H4 acetylation results in only an ~50% reduction in Bdf1 chromatin occupancy[2]. Consistent with this observation, yeast cells remain viable in the absence of acetylated residues on the H4 tail[20]; Bdf1 is recruited to immobilized promoter DNA even in the absence of nucleosomes[15,21]; a Bdf1 mutant with inactivated BDs suppresses the temperature sensitivity caused by *BDF1* deletion[18]; and chemical inhibition of BET BDs in mammalian cells neither fully displaces BET proteins from chromatin nor abolishes their function[4,5,16,22]. Together, these findings indicate that BET-mediated transcriptional regulation involves additional, yet poorly understood mechanisms that do not depend on BD activity.

BET proteins exhibit a modular architecture composed of conserved structured regions (BDs, motif B, and the extra-terminal (ET) domain) and conserved unstructured regions [the N- and C-terminal phosphorylation sites (NPS and CPS) and the basic interaction domain (BID)], interspersed with additional unstructured regions lacking sequence conservation (**Fig. 1A**). Although the functions of non-BD domains have not been comprehensively examined, existing evidence suggests that they play important roles. For instance, the ET domain of mammalian BET proteins serves as an interaction hub for multiple protein partners[17,23–25], and these interactions have been proposed to contribute to BRD4-mediated transcriptional regulation, BRD4 chromatin recruitment, and the survival of certain cancer cell lines[22,23,26–29]. However, the *in vivo* significance of the ET domain for BET protein function remains unresolved. In addition, phosphorylation within the NPS and CPS regions has been implicated in enhancing BET association with chromatin and protein partners[10,11,30]. Finally, motif B and the BID have been biochemically shown to promote BET protein dimerization[31].

Here, we delineated the contributions of the conserved domains of BET proteins to cell viability, transcription, BET chromatin association, and the recruitment and/or maintenance of partner proteins. Our key findings establish the ET domain as essential for BET protein function in living cells and enable us to propose a revised model of BET-mediated transcriptional regulation.

Results

The BET protein ET domain is essential for cell survival

Prior yeast genetic studies established that the BDs and NPS/CPS regions of BET proteins contribute to cell viability, but the functional significance of the remaining conserved domains has not been defined[18,32]. We previously demonstrated that although Bdf1 and Bdf2 have redundant roles in transcription, Bdf1 functions as the dominant BET protein in yeast[2]. Accordingly, we selected Bdf1 as our model BET factor. We generated a comprehensive collection of *BDF1* variants containing deletions or targeted mutations across all conserved BET domains. When previous work suggested functional overlap, we included combinatorial perturbations affecting more than one domain. Because intrinsically disordered regions (IDRs) have been implicated in BRD4 function in mammalian cells, we also constructed a *BDF1* variant with truncations in IDRs that do not overlap with the conserved unstructured NPS, CPS, or BID regions[33]. For the BDs and NPS/CPS regions, we introduced targeted mutations in residues required for BD function or in serine residues with documented phosphorylation, respectively[18,32]. As a comparison, we also generated a phosphomimetic *BDF1* variant in which all phosphorylated serines were substituted with glutamate. In total, we constructed eighteen *BDF1* variants (**Fig. 1B**). To facilitate stable expression in yeast cells, we cloned *BDF1* variants or unmodified *BDF1* into a minichromosomal plasmid pRS315 under the control of endogenous *BDF1* promoter and 3' untranslated region (**Table S1**).

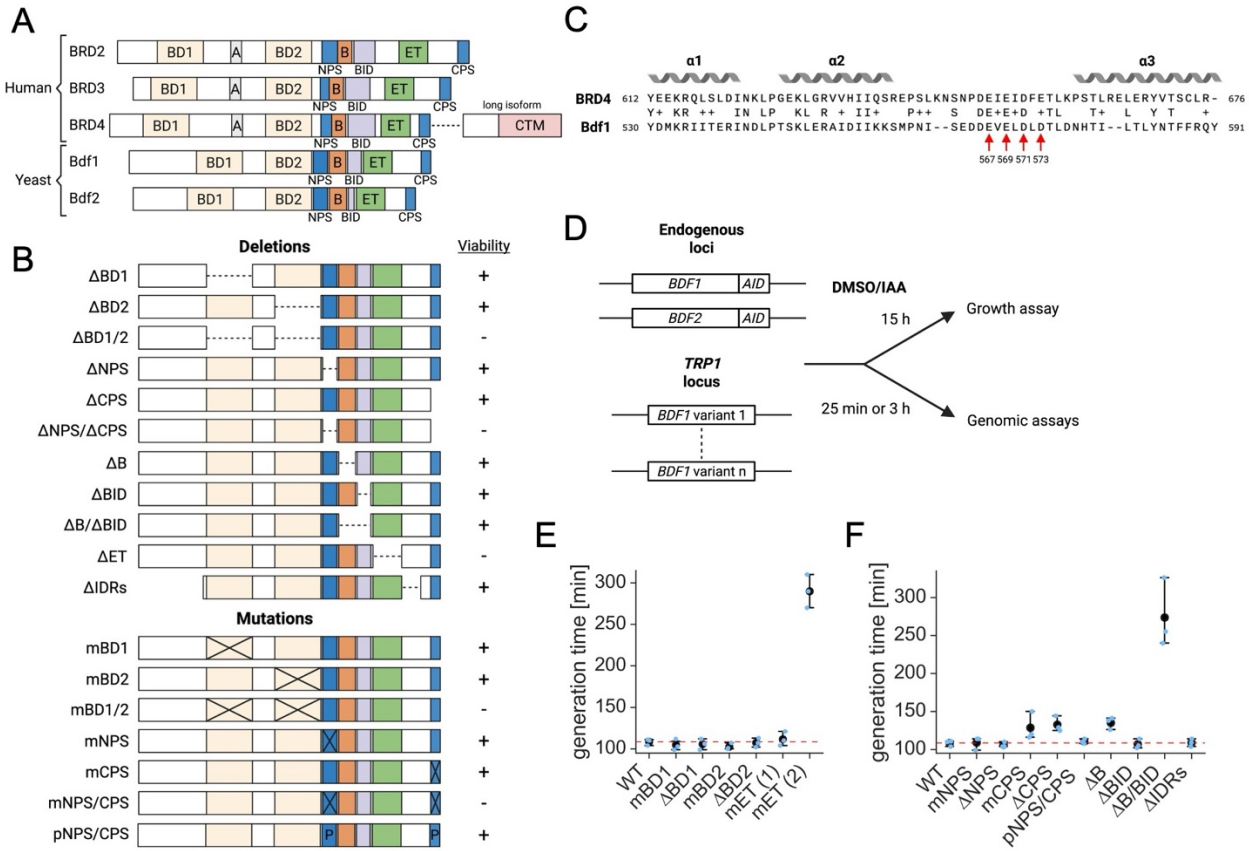

Fig. 1. **The BET protein ET domain is essential for viability.** (**A**) Conserved domain organization of BET proteins. BD – bromodomain, A/B – motifs A/B, BID – basic interaction domain, ET – extra-terminal domain, NPS/CPS – N/C-terminal phosphorylation sites, CTM – C-terminal motif (BRD4 long isoform only). (**B**) *BDF1* variants constructed in this work. Ability to support growth in the absence of endogenous *BDF1/2* is indicated. (**C**) Sequence alignment of the ET domain of BRD4 (top) and Bdf1 (bottom). Four conserved acidic residues important for interactions between BRD4 and protein partners are marked. Bdf1 coordinates are shown below the arrows. (**D**) Schematic representation of the experimental strategy for viability and genomic (SLAM-seq and ChEC-seq) assays. Experiments were performed in strains in which endogenous Bdf1/2 carried auxin-inducible degron (AID) tags and unmodified *BDF1* or *BDF1* variants were expressed from the *TRP1* locus. Endogenous Bdf1/2 were depleted by the addition of 3-indoleacetic acid (IAA). (**E-F**) Growth assays comparing the fitness of a control strain expressing unmodified *BDF1* (WT) to strains expressing *BDF1* variants after 15 h exposure to IAA (long-term loss of endogenous Bdf1/2). Black markers indicate mean generation time. Error bars represent 95% confidence intervals (n = 3).

We performed a complementation assay in a strain dependent solely on *BDF1* expressed from a minichromosomal plasmid, as endogenous *BDF1/2* were deleted. To test whether each *BDF1* variant could support viability, we attempted to replace the plasmid carrying unmodified *BDF1* and the URA3 marker with plasmids encoding the *BDF1* variants, selecting for viable transformants on medium containing 5-fluoroorotic acid (5-FOA), which counterselects URA3-

containing cells. Five *BDF1* variants failed to support viability: the double BD-deletion and BD-mutation variants, the variants lacking both NPS and CPS regions or carrying serine-to-alanine substitutions across both regions, and the variant lacking the ET domain (**Fig. 1B**). Proper expression of these *BDF1* variants was validated in experiments described below. In summary, although prior studies established *in vivo* requirements for the BDs and NPS/CPS regions of BET proteins in yeast[18,32], our findings reveal for the first time that the ET domain is essential for cell viability.

A conserved stretch of acidic residues in the ET domain is required for its function

A conserved cluster of acidic residues located between the second and third helices of the ET domain has been shown to mediate BRD4 interactions with several protein partners[23–25]. To assess the *in vivo* significance of this region in Bdf1, we generated six additional *BDF1* variants in which different numbers of four conserved acidic residues (amino acids 567, 569, 571, and 573) were substituted with alanine (**Figs. 1C and S1A**). Using the complementation assay described above, we found that mutation of three or more of these acidic residues is lethal in yeast, demonstrating that this region of the ET domain is essential for its function. For subsequent experiments, we selected a representative set of ET-domain mutants consisting of a single substitution (D571A; mET(1)), a double substitution (D571A, D573A; mET(2)), and a quadruple substitution (mET(4)) (**Figs. 1C and S1A**).

To support subsequent experiments, we integrated all *BDF1* variants, along with an unmodified *BDF1* control, into the TRP1 locus of a strain in which endogenous Bdf1/2 carry auxin-inducible degron (AID) tags (RDY73; Bdf1/2-AID strain) (**Figs. 1D, and Tables S1 and S2**)[2]. In this system, each *BDF1* variant is constitutively expressed from an ectopic locus under the control of the endogenous *BDF1* promoter and 3′ untranslated region, while endogenous Bdf1/2 can be rapidly depleted upon addition of 3-indoleacetic acid (IAA)[2]**.** Importantly, integration of an additional unmodified *BDF1* copy did not affect cell viability, and the *BDF1* variants were expressed at endogenous or modestly elevated levels, both in the presence and absence of endogenous Bdf1/2 (**Fig. S1B-D**). We did not detect expression of variants containing the BD2 deletion (ΔBD2, ΔBD1/2) or the deletion of the N-terminal unstructured region (ΔIDRs), suggesting that the antibody used recognizes epitopes located within these regions of Bdf1. Nevertheless, expression of the ΔBD2, ΔBD1/2, and ΔIDRs variants is supported by normal growth rates (ΔBD2 and ΔIDRs variants) and by the modest transcriptional changes observed in cells that rely on these *BDF1* variants, as described below.

179

180 The complementation assay identified the BET protein domains required for viability. To extend
181 these findings, we quantified growth-rate defects associated with each *BDF1* mutation. Yeast
182 cells were cultivated in the presence of IAA, forcing dependence on the Bdf1 variants as
183 endogenous Bdf1/2 were depleted, and generation times were calculated after ~15 hours of
184 growth (**Fig. 1D**). First, strains harboring *BDF1* variants that failed to support viability in the
185 complementation assay displayed complete growth inhibition, validating our earlier results.
186 Second, whereas a single point mutation in the ET domain was well tolerated, mutation of only
187 two conserved acidic residues caused a severe growth defect. By contrast, deletion or mutation
188 of a single BD did not impair growth (**Fig. 1E**). Third, we found that CPS, but not NPS, deletion
189 or mutation modestly slowed growth. Notably, the NPS/CPS phosphomimetic Bdf1 variant fully
190 supported viability, suggesting that BET proteins function optimally in a fully phosphorylated
191 state and that their phosphorylation may not be dynamically regulated under normal growth
192 conditions (**Fig. 1F**). Fourth, combined loss of the B/BID regions substantially impaired growth,
193 consistent with their proposed role in promoting BET dimerization[31]. Finally, truncation of the
194 Bdf1 IDRs did not affect viability, indicating that the large, unstructured N-terminal region of BET
195 proteins does not play a major biological role (**Fig. 1F**). As an additional validation, we observed
196 similar growth rates across all viable strains relying solely on *BDF1* variants expressed from
197 minichromosomal plasmids (**Fig. S1E and Table S2**). Collectively, these assays define the
198 contributions of all conserved BET protein domains to yeast viability and identify a critical
199 functional region within the ET domain.
200

201 **The ET domain is essential for genome-wide transcription**

202 The essential function of BET proteins is to sustain global transcriptional programs[2–5]. To define
203 the contribution of each conserved BET domain to genome-wide transcription, we analyzed our
204 collection of strains expressing *BDF1* variants in the background of endogenous Bdf1/2 fused to
205 AID tags (**Fig. 1D and Table S2**). We previously confirmed that introducing an additional
206 unmodified copy of *BDF1* does not compromise viability and that Bdf1 protein levels are
207 comparable when expressed from an ectopic versus endogenous locus (**Fig. S1B-D**). We
208 further validated that this additional *BDF1* copy does not substantially alter baseline
209 transcription and largely rescues the transcriptional defects caused by depletion of endogenous
210 Bdf1/2 (**Figs. S2A-B**). Finally, to assess whether any *BDF1* variants exert dominant-negative
211 effects in the presence of endogenous Bdf1/2, we examined growth phenotypes and found that

212 the two strains harboring variants with combined deletion or mutation of both NPS/CPS regions
213 displayed pronounced slow-growth phenotypes (**Fig. S2C**).
214
215 In contrast to the growth assay, where cells had to rely on mutant Bdf1 variants for several
216 generations, here we depleted endogenous Bdf1/2 for 25 minutes, followed immediately by 4-
217 minute labeling of newly synthesized RNA with 4-thiouracil to facilitate quantification using
218 SLAM-seq[34] (**Fig. 1D**). This approach allowed us to track direct consequences of Bdf1
219 mutations, including lethal mutations, with minimized bias from indirect effects that accumulate
220 during extended exposure to adverse genetic variants. We performed three replicate
221 experiments for all strains with (IAA) or without (dimethyl sulfoxide (DMSO)) depletion of
222 endogenous Bdf1/2 (**Table S3**). Variability in RNA levels between replicates in the final dataset
223 (see Materials and Methods) was <30–40% for most genes (**Figs. S3A-B and Table S3**). We
224 quantified transcriptional changes associated with perturbations in BET protein domains by
225 comparing strains expressing *BDF1* variants to the strain expressing unmodified *BDF1* following
226 depletion of endogenous Bdf1/2 (IAA treatment) (**Table S3**). To identify dominant-negative
227 effects, we compared strains expressing *BDF1* variants without depletion of endogenous Bdf1/2
228 to the Bdf1/2-AID parental strain (DMSO treatment), which lacks an additional *BDF1* copy (**Fig.
229 S3C and Table S3**). Consistent with the growth assay (**Fig. S2C**), strains expressing *BDF1*
230 variants with mutations or deletions in both NPS/CPS regions (mNPS/CPS and ΔNPS/CPS)
231 exhibited substantial transcriptional deviations (median change > 2-fold) in the presence of
232 endogenous Bdf1/2. We observed a similar dominant-negative phenotype for the strain
233 expressing the CPS deletion variant (ΔCPS). Consequently, we excluded ΔCPS, mNPS/CPS
234 and ΔNPS/CPS strains from further analysis and experiments.
235
236 We aligned the transcriptional changes measured following depletion of endogenous Bdf1/2
237 with those observed upon loss of Bdf1/2 in the Bdf1/2-AID strain. Surprisingly, only *BDF1*
238 variants lacking the ET domain or carrying mutations in all four conserved acidic residues of the
239 ET domain (hereafter referred to as the ET domain mutation) produced substantial
240 transcriptional defects (median decreases of 3.6-fold and 2.6-fold, respectively). By contrast,
241 deletion or mutation of both BDs resulted in relatively modest transcriptional changes (median
242 decreases of 1.5-fold and 1.4-fold, respectively) (**Figs. 2A and S4A**). Notably, the
243 transcriptional defects caused by loss of ET domain function were comparable to those resulting
244 from loss of Bdf1/2 in the Bdf1/2-AID strain (median decrease of 3.7-fold). Analysis of
245 transcriptional changes at the level of individual genes and across previously defined major

gene classes further confirmed that loss of ET domain function closely phenocopies the loss of BET proteins[35] (**Figs. 2B-C, S4B and Table S3)**. Perturbations in other domains produced only minor effects on genome-wide transcription, with the exception of the CPS mutation and the combined deletion of the B/BID regions, both of which caused moderate decreases (median decreases of 1.7-fold and 1.6-fold, respectively) (**Fig. S4A**).

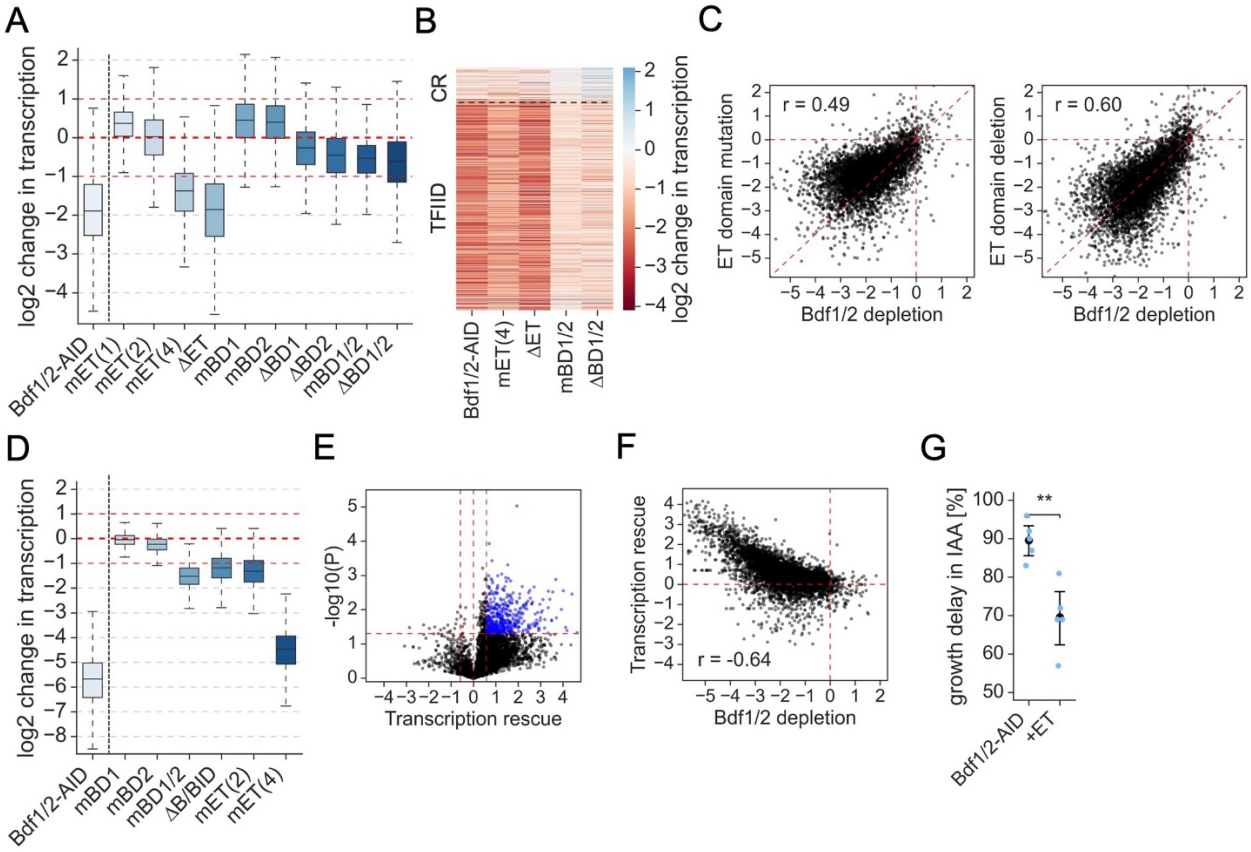

Fig. 2. **The ET domain is required for transcription of most genes.** (**A**) Log2 changes in transcription due to selected *BDF1* mutations measured by SLAM-seq after depleting endogenous Bdf1/2 for 25 min (*n* = 4,836). Results of depletion of Bdf1/2 in the absence of additional copy of *BDF1* are shown in the first sample from the left. Results for additional *BDF1* variants are shown in **Fig. S4A**. (**B**) Heatmap representation of selected results from (**A**). Genes are divided into previously defined major yeast gene classes (CR – coactivator-redundant, TFIID – TFIID-dependent)[35] (*n* = 4,560). (**C**) Comparison of selected results from (**A**). Pearson correlation coefficient (r) is shown (*n* = 4,836). (**D**) Log2 changes in transcription due to *BDF1* mutations after depleting endogenous Bdf1/2 for 3 h (*n* = 4,457). Results of depletion of Bdf1/2 in the absence of additional copy of *BDF1* are shown in the first sample from the left. (**E**) Volcano plot comparing the ability of the ET domain to rescue transcriptional changes following Bdf1/2 loss (log2 fold change over control strain) with associated *p*-values (*n* = 4,715). Thresholds used: fold change – 1.5-fold; *p*-value – 0.05 (Welch's t-test). (**F**) Comparison of ET domain-mediated rescue of transcription following Bdf1/2 loss (y-axis, log2 fold change over control strain) with gene dependence on Bdf1/2 (x-axis, log2 scale). Pearson correlation coefficient (r) is shown (*n* = 4,715). (**G**) Growth assay comparing the fitness of the Bdf1/2-AID

strain and the ET domain overexpressing strain during endogenous Bdf1/2 depletion. Samples were taken 1.5 and 3 h after DMSO or IAA addition, and growth delay was calculated by comparing generation times of IAA-treated and DMSO-treated cells. Black markers indicate mean growth delay. Error bars represent 95% confidence interval (n = 5). Results of a Welch's t-test are shown (** – p-value < 0.01).

A modest change in transcription following BD inactivation was unexpected given the lethal phenotype associated with this mutation. We observed a similar discrepancy for deletion of the B/BID regions and mutation of two conserved acidic residues in the ET domain, both of which produced severe growth defects yet only minor transcriptional changes. To validate these findings, we extended the depletion period of endogenous Bdf1/2 to 3 hours to assess the accumulation of indirect effects on transcription. After 3 hours of IAA treatment, the Bdf1/2-AID strain exhibited a near-complete loss of genome-wide transcription (median decrease of 51-fold) (**Fig. 2D and Table S3**). In contrast, BD1/2 mutation, ET domain double mutation, and B/BID deletion resulted in more modest median decreases of 2.9-fold, 2.5-fold, and 2.3-fold, respectively. Compared to the rapid depletion experiment (**Figs. 2A and S4A**), these results indicate that the viability defects associated with BD1/2 mutation, the ET domain double mutation, or B/BID deletion arise primarily from indirect transcriptional dysfunction. Nevertheless, the indirect effects observed after 3 hours of IAA treatment were substantially stronger for the ET domain quadruple mutation (median decrease of 22.3-fold), consistent with trends observed following 25-minute depletion of endogenous Bdf1/2. In comparison, mutation of individual bromodomains did not appreciably affect transcription after prolonged IAA treatment, consistent with the minimal viability defects associated with these *BDF1* variants.

Based on our findings, we hypothesized that the ET domain can at least partially compensate for the loss of BET proteins. To test this hypothesis, we overexpressed the ET domain in the Bdf1/2-AID strain (**Fig. S4C**) and quantified transcriptional changes following 25 minutes of induced Bdf1/2 depletion. First, we observed that very few genes exhibited substantial transcriptional changes as a result of ET domain overexpression in the presence of endogenous Bdf1/2 (**Fig. S4D-E and Table S3**). Next, we compared transcriptional responses to Bdf1/2 loss between the ET domain overexpressing strain and the parental Bdf1/2-AID strain. We found that the ET domain compensated for the loss of BET proteins at many genes, with 455 genes showing statistically significant transcriptional rescue (**Fig. 2E and Table S3**). Notably, this effect was most pronounced at strongly Bdf1/2-dependent genes (**Fig. 2F**). Consistent with these observations, the ET domain partially rescued the growth phenotype associated with BET protein loss, although prolonged exposure to IAA ultimately remained lethal (**Fig. 2G**). In

305 summary, these results reveal a surprisingly small direct contribution of the BDs to transcription
306 and demonstrate that the ET domain is a dominant BET protein domain in transcriptional
307 regulation.
308
309 **The ET domain facilitates BET protein recruitment to chromatin**
310 To modulate transcription, BET proteins first need to be recruited to gene regulatory elements.
311 Experiments in both yeast and mammalian cells have shown that BD function does not fully
312 account for BET protein chromatin occupancy[2,4,15,16,22]. To identify BET protein domains that
313 contribute to Bdf1 recruitment to chromatin, we modified selected yeast strains used in the
314 SLAM-seq experiments by inserting a micrococcal nuclease (MNase) coding sequence before
315 the stop codon of *BDF1* variants to facilitate ChEC-seq analysis (**Tables S1 and S2**)[36]. We
316 previously found that ChEC-seq complements and outperforms ChIP-seq for mapping BET
317 protein chromatin occupancy in yeast[2]. First, we validated that ectopically expressed Bdf1-
318 MNase supports normal growth in the presence of AID-tagged endogenous *BDF1*/2 (**Fig. S5A**).
319 We also confirmed that ectopically expressed Bdf1-MNase displays a chromatin-binding pattern
320 highly similar to that of Bdf1-MNase expressed from the endogenous locus, both in the
321 presence and absence of endogenous Bdf1/2 (**Fig. S5B**). As in the SLAM-seq assays, sample
322 collection was preceded by a 25-minute depletion of endogenous Bdf1/2 to minimize
323 confounding effects from endogenous BET proteins. All experiments were performed in three
324 biological replicates, and the replicate datasets were highly consistent (**Fig. S5C**).
325
326 To evaluate the impact of targeted mutations in BET protein domains on Bdf1 recruitment, we
327 compared data collected from strains expressing *BDF1* variants to that from the control strain
328 expressing unmodified *BDF1* in the context of endogenous Bdf1/2 depletion (IAA treatment)
329 (**Table S4**). Consistent with the major impact of the ET domain on transcription, we found that
330 this domain broadly contributed to *Bdf1* chromatin occupancy (**Figs. 3A-C**). Surprisingly, at
331 most gene promoters, the contribution of the ET domain to Bdf1 occupancy exceeded that of
332 the BDs. Notably, deletion of the BDs or the ET domain produced very similar effects (**Figs. 3D**
333 **and S6A-C**). Among other domains, perturbations in the CPS domain and the B/BID regions
334 also affected Bdf1 recruitment, indicating that BET protein phosphorylation and dimerization
335 both contribute to establishing genome-wide BET occupancy (**Fig. S6D-F**). None of the
336 examined mutations caused substantial redistribution of Bdf1 to new loci. Next, we compared
337 changes in Bdf1 promoter recruitment resulting from mutation of the BDs or the ET domain with
338 levels of histone H4 lysine 12 acetylation (H4K12ac), a preferred target of Bdf1 BDs[19]. As

expected, changes in Bdf1 recruitment due to BD mutation showed a modest correlation with H4K12ac levels, consistent with prior findings that BD inhibitors preferentially evict BET proteins from loci with high H4 acetylation, such as super enhancers[4]. In contrast, the effects of the ET domain on Bdf1 occupancy were independent of promoter acetylation levels (**Fig. 3E**). Finally, we observed only a weak correlation between changes in Bdf1 recruitment and transcriptional output (**Fig. S6G**), consistent with the previously reported lack of correlation between baseline Bdf1 promoter occupancy and transcription[2]. In summary, we revealed that the ET domain, not the BDs, is the primary contributor to the BET protein chromatin occupancy.

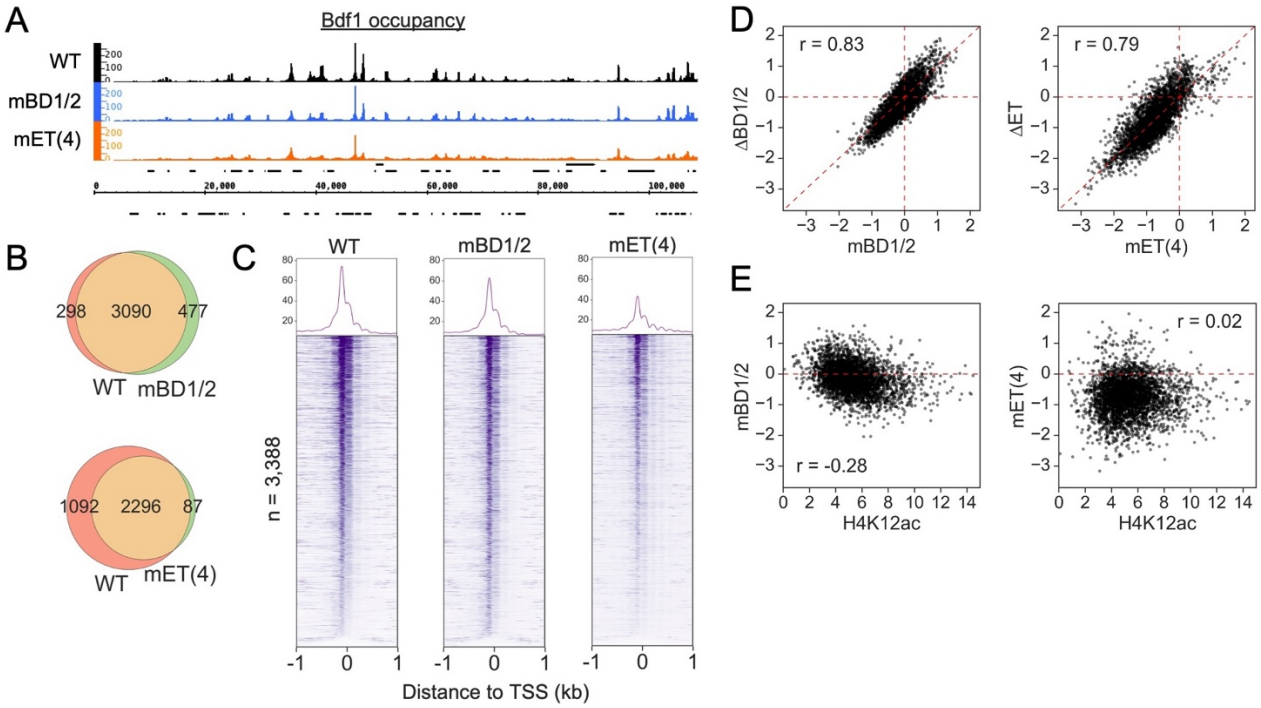

Fig. 3. **The ET domain has a major role in facilitating BET protein recruitment to chromatin.** (**A**) Genome browser snapshot showing the binding patterns of unmodified Bdf1 (WT) and Bdf1 variants with mutations in the BDs or the ET domain as determined by ChEC-seq. Data for the first 100,000 bases of chromosome III are shown. (**B**) Overlap of Bdf1-bound promoters for the indicated experiments. (**C**) Occupancy of unmodified Bdf1 and Bdf1 variants with mutations in the BDs or the ET domain around the transcription start sites (TSS) of 3,388 genes whose promoters are bound by unmodified Bdf1. Genes are sorted by the TSS signal (+/- 200 bp) in the WT experiment. (**D**) Comparison of log2 changes in Bdf1 occupancy due to mutation or deletion of the BDs or the ET domain. Bdf1 occupancy was calculated as the sum of signal within the (-100, 100) bp window around the Bdf1 promoter peak summit. Pearson correlation coefficient (r) is shown (*n* = 3,388). (**E**) Comparison of H4K12ac level at promoters [2] and log2 changes in Bdf1 occupancy due to mutations in the BDs or the ET domain. Pearson correlation coefficient (r) is shown.

364 **The ET domain supports TFIID recruitment to gene promoters.**
365 Both yeast and mammalian BET proteins have been linked to the coactivator TFIID, which
366 regulates transcription initiation[2,14,15]. Our prior work demonstrated that Bdf1/2 are required for
367 transcription initiation, and that loss of Bdf1/2 modestly decreases TFIID promoter occupancy[2].
368 Building on this background and our new findings, we hypothesized that a major function of the
369 ET domain in transcription regulation is to facilitate TFIID recruitment. To test this hypothesis,
370 we applied ChEC-seq to quantify changes in TFIID occupancy in cells relying solely on Bdf1
371 variants after rapid depletion of endogenous Bdf1/2. We inserted an MNase coding sequence
372 into the TFIID subunit Taf1 in three strains previously used in the SLAM-seq assays: the control
373 strain carrying an unmodified additional copy of *BDF1*, and strains carrying *BDF1* variants with
374 mutations in the ET domain or the BDs (mET(4) and mBD1/2, respectively). After depleting
375 endogenous Bdf1/2, we quantified changes in Taf1 recruitment by comparing strains expressing
376 *BDF1* variants to the control strain. Experiments were performed in three biological replicates,
377 and the replicate datasets were highly reproducible (**Fig. S7A**). We found that both the ET
378 domain and the BDs contributed to TFIID recruitment to promoters; however, the ET domain
379 contributed more prominently at most loci (**Fig. 4A-B**). Next, we compared changes in TFIID
380 occupancy resulting from Bdf1 mutations with changes in transcription and observed only a
381 modest correlation (**Fig. S7B**). Consistent with this finding, we previously reported that
382 transcription is uncoupled from baseline TFIID promoter occupancy, and that changes in TFIID
383 occupancy due to complete loss of BET proteins do not correlate with transcriptional output[2,35].
384 In summary, our results demonstrate that the ET domain plays a major role in TFIID recruitment
385 to gene promoters.

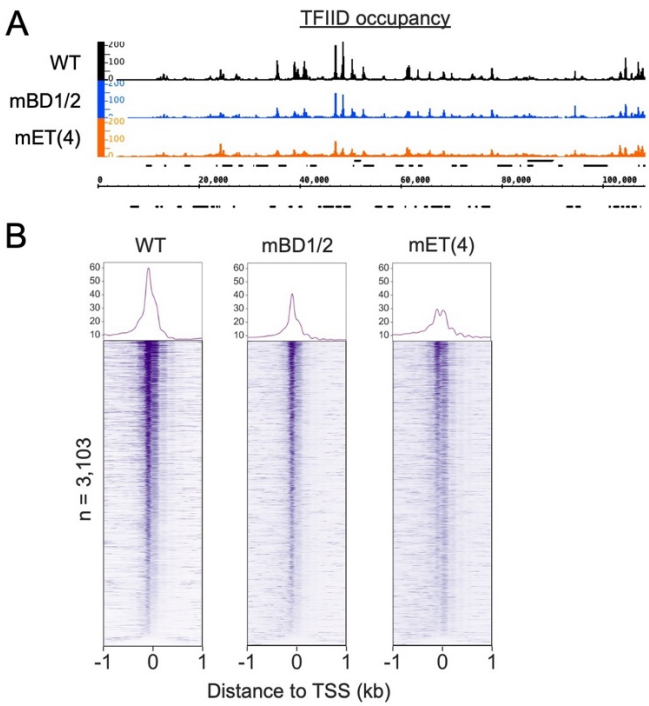

Fig. 4. **The ET domain facilitates recruitment of TFIID to promoters.** (**A**) Genome browser snapshot showing Taf1 (TFIID) binding pattern in the context of unmodified Bdf1 or Bdf1 variants with mutations in the BDs or the ET domain as determined by ChEC-seq. Data for the first 100,000 bases of chromosome III are shown. (**B**) Taf1 occupancy around TSS of 3,103 genes whose promoters are bound by Taf1[2], in the context of unmodified Bdf1 or Bdf1 variants with mutations in the BDs or the ET domain. Genes are sorted by the signal around TSS (+/- 200 bp) in the WT experiment.

The ET domain engages its targets using a conserved mechanism

Results described thus far show that the ET domain is a primary functional module of Bdf1 and that its impact on transcription is at least partially explained by its role in facilitating TFIID recruitment. Consistent with the latter finding, the ET domain of BRD4 has been proposed to modulate transcription by mediating interactions with protein partners[17,22,23]. However, only a limited number of interactions involving the ET domain of mammalian BET proteins have been experimentally validated, and it remains unknown how many factors associate with the ET domain or what the functional consequences of those interactions are. To begin addressing these questions, we used chromatin mass spectrometry (chromatin-MS) to identify candidate factors – beyond TFIID – that may depend on Bdf1/2 for recruitment to chromatin. We obtained reliable data for 724 of 2399 yeast nuclear proteins and found that 78 exhibited decreased chromatin association following rapid Bdf1/2 depletion. As validation of our approach, this list included two TFIID subunits. Notably, we also identified additional proteins implicated in

transcription regulation, including Bur1/CDK9, Spt6, the PAF1 complex (PAF1C) subunit Rtf1, subunits of the RSC, INO80, and ISW2 chromatin remodeling complexes, and several factors involved in mRNA processing (**Figs. 5A and S8A and Table S5**).

Based on proteomic and structural biology studies, the BRD4 ET domain has been proposed to recognize two consensus motifs – Φ[+]Φ[+] or (Φ/[+])ΦΦ[+](Φ/[+]), where Φ is M, L, V, I, or F and [+] is K or R – referred to here as ET-interacting motifs (ETMs)[17,24,25]. Screening the yeast nuclear proteome revealed 2418 ETMs in 1253 proteins, including 60 of the 78 proteins identified in our chromatin-MS experiment (**Fig. 5B and Table S6**). Given this large number of putative interactors, we used AlphaFold2 to model interactions between the Bdf1 ET domain and candidate ETMs[37]. As an initial validation of this approach, we modeled the BRD4 ET domain with selected partner peptides and observed strong similarity between the predicted structures and published experimental structures, including formation of an interfacial β-sheet involving the unstructured loop between the α2 and α3 helices of the ET domain, which adopts a β-strand configuration when bound to partner peptides (**Fig. S8B-C**). Modeling the Bdf1 ET domain with the same peptides similarly produced structures consistent with experimental data, including conditional interfacial β-sheet formation, suggesting a conserved mode of interaction (**Fig. S8D**). We next folded the Bdf1 ET domain with each of the 2418 ETMs identified in yeast nuclear proteins using two implementations of AlphaFold2 and scored models using multiple confidence metrics and interfacial β-sheet establishment (see Materials and Methods) (**Table S7**). To test whether our approach could identify bona fide ET domain interactors, we focused on the TFIID subunit Taf7, a confirmed Bdf1-interacting partner. The interaction was previously mapped to the N-terminal 100 amino acids of Taf7[15]. Within this region, we identified four putative ETMs, each ranking highly in accessibility and model confidence (**Figs. 5C and S8E-F and Table S7**). Structural models of these four ETMs in complex with the Bdf1 ET domain were well supported and showed conditional interfacial β-sheet formation (**Figs. 5D and S9A**). Using a yeast two-hybrid system, we tested whether the Bdf1-Taf7 interaction is mediated by the ET domain and by ETMs in the Taf7 N-terminal region. We found that the Bdf1 ET domain interacts with Taf7 and that this interaction was abolished either by mutating the ET domain or by substituting basic residues with alanine in all four Taf7 ETMs (**Fig. 5E**). Based on these results, together with the observation that conditional β-sheet formation correlates with higher model confidence (**Fig. S9B-C**), we defined 770 high-confidence ETMs (AlphaFold RSA ≥ 0.24 and FoldScore = 1) present in 596 nuclear proteins (**Table S7**). This high-confidence ETM-containing set was enriched for proteins previously associated with Bdf1 function (**Fig. S9D**).

Taken together, these findings provide a mechanistic basis for Bdf1-dependent recruitment of TFIID, demonstrate that the ET domains of yeast and mammalian BET proteins engage their targets using a conserved interaction mechanism, and validate our approach for systematically identifying and characterizing interacting partners of the BET protein ET domain.

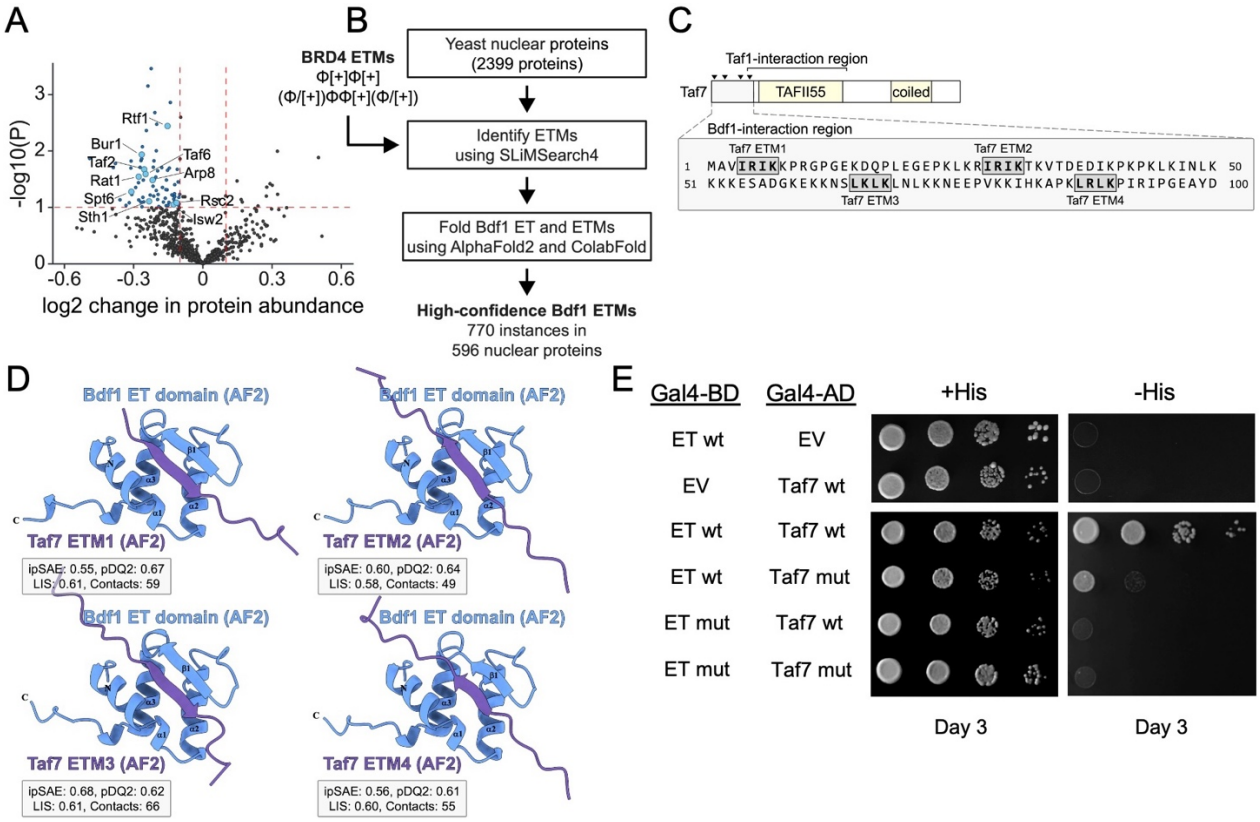

Fig. 5. The ET domain of yeast and mammalian BET proteins uses the same mechanism to engage its targets. (**A**) Volcano plot comparing –log10 *p*-value and log2 change in abundance for chromatin-associated proteins following Bdf1/2 depletion. Data for reliably detected nuclear proteins are shown (*n* = 724). (**B**) Schematic representation of the experimental strategy for identifying high-confidence ET-interacting motifs (ETMs) in *S. cerevisiae* nuclear proteins. (**C**) Functional domains of Taf7. Interaction with Bdf1 was previously mapped to the unstructured N-terminal region of Taf7 [15], which contains four high-confidence ETMs (detail). The TAFII55 region mediates interaction with Taf1 and is conserved across Taf7 homologs in other eukaryotes. The predicted C-terminal coiled-coil domain is poorly characterized. Other regions of Taf7 are largely unstructured. (**D**) AlphaFold2 (AF2) predicted structures for the Bdf1 ET domain in association with four putative ETMs in the Bdf1-interaction region of Taf7. Confidence metrics (ipSAE, pDockQ2, and LIS) and the number of interfacial contacts supporting structural predictions are shown. (**E**) Y2H analysis of the interaction between the Bdf1 ET domain and Taf7. Plasmids expressing the Bdf1 ET domain (WT or mut), Taf7 (WT or mut), or empty vector (EV) were co-transformed into the host strain. Cells were serially diluted, spotted on indicated media, and imaged after three days of growth (*n* = 3). ET mut – ET domain with four conserved acidic residues substituted with alanine. Taf7 mut – Taf7

467 with basic residues in the four ETMs in the N-terminal region (first 101 amino acids[15])
468 substituted with alanine.
469

470 **Multiple interactions mediated by the ET domain contribute to gene transcription**

471 To further define the mechanistic basis by which the ET domain regulates transcription, we
472 selected the TFIID subunit Taf7 and several additional regulatory factors for detailed analysis.
473 Specifically, we focused on Bur1/CDK9, Spt6, the PAF1C subunit Rtf1, two conserved mRNA-
474 processing factors (Rat1/XRN2 and Rna14/CSTF3), and Pob3, a subunit of the histone
475 chaperone FACT. Each of these proteins contains at least one high-confidence ETM (**Fig. S10**
476 **and Table S7**), and all except Pob3 showed decreased chromatin association following Bdf1/2
477 depletion in our chromatin-MS experiment (**Fig. 5A**). Notably, both FACT subunits Pob3 and
478 Spt16 were previously identified as putative Bdf1-associated proteins by mass spectrometry[18],
479 and CDK9, FACT, SPT6, PAF1C, XRN2 and CSTF3 have been linked to BET proteins in
480 mammalian cells[5,13,22,38]. However, the mechanistic basis of an association involving BET
481 proteins and any of these factors except CDK9 has not been established.
482

483 We first used parallel reaction monitoring mass spectrometry (PRM-MS), a highly quantitative
484 MS method that targets predefined peptides[39], to measure changes in chromatin association of
485 Bur1, FACT, Spt6, PAF1C, Rat1, and Rna14 following Bdf1/2 depletion. Because Rtf1 could not
486 be reliably detected by PRM-MS, we instead quantified changes in Paf1, the major subunit of
487 PAF1C. For all factors tested, we observed an approximately 50% loss of chromatin
488 association, without a corresponding decrease in total protein levels (**Fig. 6A and Table S5**).
489 Second, we used a yeast two-hybrid system to test interactions between predicted high-
490 confidence ETMs in Bur1, Pob3, and Spt6 (**Fig. S10 and Table S7**) and the ET domain of Bdf1.
491 We found that the Bdf1 ET domain interacted with all predicted targets and that, with the
492 exception of one Pob3 ETM, these interactions were abolished by mutation of either the ET
493 domain or the ETMs (**Fig. S11A**). Based on these results, we generated yeast strains stably
494 expressing variants of Taf7, Bur1, Spt6, or Pob3 in which all identified ETMs were mutated by
495 substituting lysine or arginine residues with alanine. All ETM-mutant strains exhibited moderate
496 growth defects, indicating the functional importance of ET-mediated interactions with the
497 analyzed factors (**Fig. 6B**). Next, we applied SLAM-seq to determine whether ETM-mutant
498 strains display alterations in transcriptional programs (**Table S3**). In the case of the Taf7 and
499 Bur1 mutant strains, we observed downregulation of large subsets of genes (**Fig. 6C**).
500 Conversely, we detected upregulation of many genes in the the Pob3 and Spt6 mutant strains
501 (**Fig. 6C**), suggesting that the interactions between BET proteins and FACT or Spt6 are

important for reducing and/or fine-tuning the transcription of certain genes. Consistent with this interpretation, prior studies reported increased coding transcription of subsets of genes upon impaired FACT or Spt6 function[40–42]. Importantly, across all ETM-mutant strains, the subsets of genes that passed the significance threshold overlapped with genes that are strongly sensitive to Bdf1/2 loss (**Fig. S11B**). In summary, our findings demonstrate that ET domain–mediated interactions of BET proteins support chromatin occupancy of multiple partner proteins and enable optimal transcription of target genes.

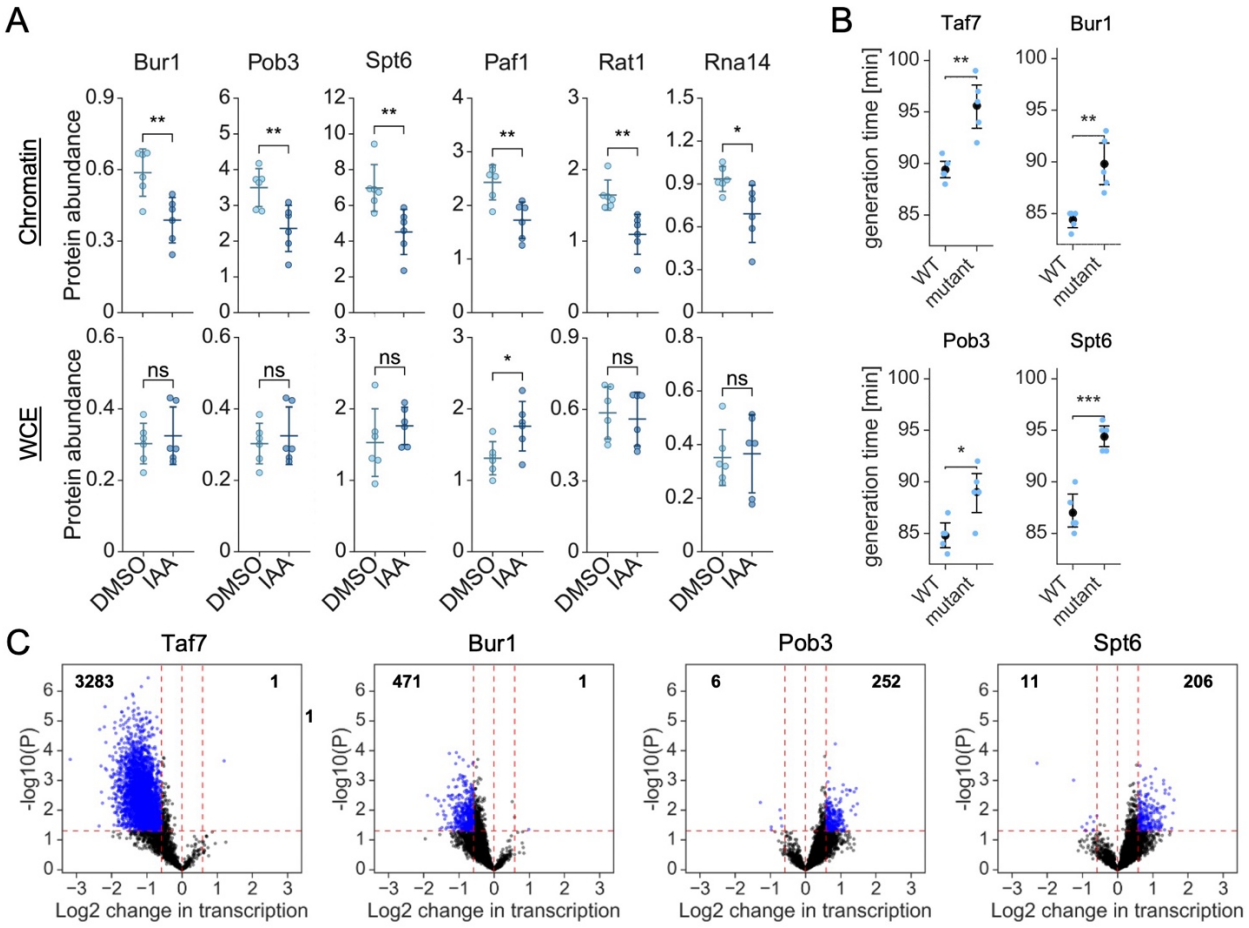

Fig. 6. The ET domain modulates transcription by recruiting key regulatory factors. (**A**) Abundance of selected proteins in chromatin-enriched fractions (top panel) or whole cell extract (bottom panel) following Bdf1/2 depletion as determined by parallel reaction monitoring mass spectrometry. Central lines indicate mean protein abundance. Error bars represent standard deviation of the mean (n = 6). Results of a Welch's t-test are shown (* – p-value < 0.05, ** – p-value < 0.01, ns – not significant). (**B**) Growth assays comparing the fitness of strains expressing variants of indicated proteins carrying targeted ETM mutations to control strains expressing a wild-type variant of the protein from the same genomic locus. Black markers indicate mean generation times. Error bars represent 95% confidence interval (n = 5). Results of a Welch's t-test are shown (* – p-value < 0.05, ** – p-value < 0.01, *** – p-value < 0.001). (**C**)

521 Volcano plots showing log2 change in transcription due to mutation of ETMs in indicated
522 proteins (n = 4,498). The numbers of genes showing significant up- or down-regulation are
523 indicated. Thresholds used: fold change – 1.5-fold; p-value – 0.05 (Welch's t-test).
524
525
526
527 **Discussion**
528 Discovery of specific inhibitors of BET BDs brought the promise of effective treatments for
529 cancer and other diseases. However, the clinical application of BD inhibitors has faced
530 significant challenges due to emerging resistance, cellular heterogeneity, and an incomplete
531 understanding of BET protein biology. In this work, we used a highly versatile yeast model
532 system to define the contributions of all conserved BET protein domains to cell viability, gene
533 transcription, and BET chromatin occupancy. We found that the ET domain, rather than the
534 BDs, constitutes the primary functional module of BET proteins. These results both complement
535 and challenge existing models of BET-mediated transcription, reconcile conflicting observations
536 from prior studies, and suggest new directions for future research.
537
538 Many studies have reported BET protein recruitment and function that persist despite BD
539 inhibition[5,10–12,22]. Through genetic analysis, we identified five BET protein domains essential for
540 cell viability, including the BDs, the ET domain, and the phosphorylated NPS/CPS regions.
541 Although the requirement for at least one BD and for the NPS/CPS regions was previously
542 established[18,32], our work is the first to demonstrate that the ET domain is essential for cell
543 survival. Consistent with the viability defects, we found that the ET domain makes major
544 contributions to global transcription and to BET protein recruitment to chromatin, exceeding the
545 contributions of the BDs. In addition, guided by prior studies[23–25], we identified conserved acidic
546 residues required for ET domain function *in vivo*. The ET domain has been proposed as a
547 feasible drug target for modulating aberrant transcription in human disease[17,28,29]. Structural
548 information for the ET domain in complex with selected peptide ligands is available, and our
549 data show that the mechanistic basis of ET-mediated interactions is conserved between yeast
550 and mammals. Thus, the yeast model system can serve as a valuable platform to evaluate the
551 ability of small-molecule inhibitors to disrupt ET domain function. Importantly, relative sensitivity
552 of cancer cells to BD inhibition or BET protein degradation differs depending on the tissue of
553 origin and other characteristics, suggesting a possibility of tailored therapeutic approaches[4,8,10].
554 Altogether, our findings provide a framework and rationale for developing approaches to

555 modulate BET protein activity by targeting the ET domain either in place of, or in combination
556 with, BD inhibition.
557
558 Other phenotypes we observed for Bdf1 mutants also complement and extend prior studies.
559 Motif B and the BID were shown to facilitate BRD4 dimerization in biochemical assays, and
560 deletion of motif B caused dissociation of BRD2 from chromatin[31,43]. We observed a significant
561 growth phenotype correlated with changes in Bdf1 recruitment and, to a lesser extent, changes
562 in transcription resulting from deletion of the B/BID regions. Together with prior studies, these
563 findings indicate that BET proteins function as dimers, and future work should address how
564 dimerization modulates BET protein recruitment and activity. For example, an important
565 regulatory layer may arise from the relative ability of BET proteins to form homo- and
566 heterodimers. Phosphorylation of BET proteins in the NPS and CPS regions has been linked
567 with resistance to BD inhibition, interactions with protein partners, and the propensity of BET
568 proteins to dimerize[10,11,30,31]. It was proposed that NPS/CPS phosphorylation may act as a
569 switch that modulates BET protein dimerization and affinity for distinct partners[30,31]. In contrast,
570 our finding that a phosphomimetic *BDF1* variant supports normal growth and causes only mild
571 changes in transcription and Bdf1 chromatin occupancy suggests that dynamic regulation of
572 BET protein phosphorylation is not required for BET protein function. Moreover, prior work
573 proposed distinct roles for the NPS and CPS regions, with NPS phosphorylation linked to BD
574 activity and CPS phosphorylation suggested to influence ET domain function[10,30]. We found that
575 mutation or deletion of NPS did not impair BET protein function, mutation or deletion of CPS
576 was detrimental, and simultaneous perturbation of both regions was lethal. Based on these
577 observations, we propose that phosphorylation of the NPS and CPS regions supports the same
578 functional role or roles of BET proteins. Nevertheless, the biological significance of BET protein
579 phosphorylation remains unresolved and warrants further investigation.
580
581 Two recent studies provided mechanistic explanations for BD-independent functions of
582 mammalian BET proteins in transcription[5,22]. Zheng *et al.*[5] demonstrated that the C-terminal
583 fragment specific to the long isoform of BRD4 can independently promote the release of paused
584 RNA polymerase II (Pol II) through interaction with CDK9/CCNT1 (the P-TEFb complex) and
585 can rescue transcription of a subset of genes following depletion of endogenous BRD4. Yeast
586 lack an equivalent of the long BRD4 isoform, and transcription in yeast does not involve a
587 regulated Pol II pause-and-release mechanism. Our experiments demonstrated that the Bdf1
588 ET domain interacts with the CDK9 homolog Bur1, and that mutation of Bur1 ETMs impairs cell

589 growth and transcription of a subset of genes. As additional validation, we previously reported
590 defects in Pol II processivity at many of the same genes following Bdf1/2 depletion[2]. Taken
591 together, these observations support a conserved association between BET proteins and
592 Bur1/CDK9 in yeast and mammals, even though the mechanistic basis of the interaction differs.
593 In yeast, the roles of BET proteins in transcription initiation and elongation are mediated
594 primarily by a single Bdf1 isoform and likely by the same functional domain, the ET domain. In
595 mammalian cells, evolutionary acquisition of the long BRD4 isoform may reflect the need to
596 separate BRD4 functions in transcription elongation from other activities also mediated by the
597 short BRD4 isoform, which may be shared with BRD2 and BRD3[14,17,23]. Why such functional
598 separation became advantageous in the context of more complex gene regulatory networks
599 remains an important question for future investigation.
600
601 Zhang *et al.*[22] reported that BRD4 activates transcription at estrogen receptor binding sites
602 through BD-independent associations with SPT5, SPT6, and PAF1C. Consistent with this
603 finding, we observed that Bdf1/2 depletion reduces chromatin association of Spt6 and PAF1C.
604 Spt5, Spt6, and PAF1C subunits each contain high-confidence ETMs, and mutation of Spt6
605 ETMs resulted in growth defects and dysregulated transcription at many Bdf1/2-dependent
606 genes. Zhang *et al.*[22] also showed that association with the transcriptional coactivator Mediator
607 contributes to BD-independent BRD4 recruitment. Importantly, the mechanistic basis of the
608 established association between BET proteins and Mediator remains unresolved. Because
609 several Mediator subunits are present in our high-confidence ETM list, it is plausible that BET
610 proteins directly interact with Mediator via the ET domain. Finally, although Bdf1/2 depletion
611 modestly reduces Mediator chromatin occupancy[2], Bdf1 chromatin association may also be
612 regulated by interactions with Mediator, consistent with the substantial loss of Bdf1 chromatin
613 occupancy observed upon ET domain mutation.
614
615 In summary, we provided evidence that the ET domain has a critical role in transcription by
616 serving as a hub for interactions with multiple protein partners, including the transcription
617 coactivator TFIID, Bur1/CDK9, and the histone chaperones Spt6 and FACT. Our analysis
618 indicates that the repertoire of direct ET domain interactors is likely substantially larger. The
619 experimental framework described here can be applied to identify and functionally characterize
620 ET domain interactions with additional transcription regulators in both yeast and mammalian
621 cells. We propose that multiple protein-protein interactions mediated by the ET domain facilitate
622 recruitment of diverse components of the transcription machinery, as well as recruitment of BET

proteins themselves. Importantly, this model is consistent with current views of transcription regulation based on the formation of transcriptional condensates through transient interactions among multivalent proteins, and with the propensity of BET proteins to promote condensate formation at gene regulatory elements[44,45].

Despite fundamental and clinical relevance, many aspects of the biology of BET proteins remain poorly understood. We revealed critical roles of the BET protein ET domain in sustaining global transcription and facilitating BET protein recruitment to chromatin. Our findings provide a new mechanistic explanation for the failure of BD inhibitors to abolish BET protein chromatin occupancy and function in clinical settings and suggest directions for future investigations toward a comprehensive model of the complex roles of BET proteins in transcription regulation.

Limitations of the study

First, the experiments described in this study were carried out under optimal growth conditions (rich medium, 30°C). As such, it remains to be determined if the contributions of distinct BET protein domains to transcription vary depending on the nutrient availability, stress, or external signaling cues. Second, although prior evidence suggests that Bdf1 is the primary BET protein in yeast cells[2,15], we cannot exclude the possibility that Bdf2 plays important and non-redundant roles in transcription that are not addressed by our experiments. For example, Bdf2 may be necessary for gene activation rather than steady-state transcription, analogous to proposed roles for BRD2 and BRD3 in mammalian cells [46]. Consistent with this idea, our recent study identified the *BDF2* promoter as a target of numerous sequence-specific transcription factors, the *BDF2* gene was shown to be regulated by two distinct RNA degradation mechanisms in response to environmental conditions, and Bdf2 was among a small subset of yeast proteins with an unusually short half-life, suggesting dynamic regulation of *BDF2* expression transcriptionally, post-transcriptionally, and post-translationally[47–49]. Finally, there is a possibility that small amounts of endogenous Bdf1/2 remaining after depletion using the AID system may have contributed to confounding effects in our experiments, potentially biasing our interpretation. However, we consider this unlikely, as we observed highly similar results between growth retardation experiments based on Bdf1/2 depletion and *BDF1/2* gene deletion, in which growth was supported by *BDF1* variants expressed from minichromosomal plasmids.

Materials and Methods

657 **Yeast cell growth**

658 All *Saccharomyces cerevisiae* and *Schizosaccharomyces pombe* strains used in this study are
659 listed in Table S2. For strain construction, *S. cerevisiae* strains were grown in YPD medium (1%
660 yeast extract, 2% peptone, 2% glucose, 20 µg/ml adenine sulfate) or in synthetic complete (SC)
661 media (0.17% yeast nitrogen base without ammonium sulfate or amino acids [BD Difco], 0.5%
662 ammonium sulfate, 40 µg/ml adenine sulfate, 0.6 mg/ml amino acid dropout mix, supplemented
663 with 2 µg/ml uracil and 0.01% other amino acids to complement auxotrophic markers) at 30°C.
664 Standard amino acid dropout mix contains 2 g each of Tyr, Ser, Val, Ile, Phe, Asp, and Pro and
665 4 g each of Arg, Thr, Lys, and Met. 1.5% Bacto-agar (BD Difco) was added to medium as
666 required for growth on solid media. For complementation assays, *S. cerevisiae* strains were
667 grown in SC medium lacking Leu to select for cells carrying a minichromosomal plasmid with
668 *BDF1* variants and plated onto medium containing 5-fluoroorotic acid (5-FOA) to shuffle out the
669 wild-type *BDF1* plasmid carrying the URA3 marker. For genomic and growth assays, *S.*
670 *cerevisiae* cells were grown in YPD medium at 30°C with shaking. *Schizosaccharomyces*
671 *pombe* cells were grown in YE medium (0.5% yeast extract, 3% glucose) at 30°C with shaking.
672 In experiments involving degron-mediated depletion of target proteins, cells were treated with 1
673 mM IAA dissolved in DMSO, or with DMSO alone, for 25 min or 3 h to induce protein
674 degradation, followed by protocol-specific steps. For SLAM-seq and ChEC-seq experiments, *S.*
675 *cerevisiae* cells were collected between an OD600 of 0.5 and 0.7, and *S. pombe* cells were
676 collected at an OD600 of 1.0. For growth assays, cells were grown from an OD600 of 0.0001–
677 0.0005 for 15 h with or without addition of IAA or DMSO. A minimum of five biological replicates
678 were collected for growth assays using strains expressing *BDF1* variants from a
679 minichromosomal plasmid. Three biological replicates were collected for all other experiments
680 unless otherwise indicated.

681

682 **Plasmid and strain construction**

683 Plasmids and *S. cerevisiae* strains were constructed using standard methods and are described
684 in **Tables S1 and S2**, respectively. Previously described plasmids or strains were used as
685 indicated[36,50–52]. Proteins were chromosomally tagged by yeast transformation and homologous
686 recombination of PCR-amplified DNA. For ChEC-seq experiments, proteins were tagged with
687 3xFLAG-MNase::TRP1 or 3xFLAG-MNase::HYG using pGZ110[36] or pMD75 (this work)
688 plasmids, respectively.

689

690 **ET domain overexpression**

691 The gene fragment encoding the Bdf1 ET domain was cloned into the pMD1 plasmid under the
692 control of the *GPM1* promoter and the *BDF1* terminator and placed in frame with the *RPL25*
693 nuclear localization signal and a 3xV5 epitope. The resulting plasmid pJR15 was integrated into
694 the *TRP1* locus of strain RDY73 (Bdf1/2-AID) to generate strain RDY388.
695
696 **Western blot analysis**
697 A 1 ml fraction of culture was collected and pelleted from strains after treatment with IAA or
698 DMSO, washed with 500 µl water, and resuspended in 100 µl of yeast whole cell extract buffer
699 (60 mM Tris-HCl [pH 6.8], 10% glycerol, 2% SDS, 5% 2-mercaptoethanol, 0.0025%
700 bromophenol blue). After heating at 95°C for 5 min, samples were centrifuged at 21,000 × g for
701 5 min and analyzed by SDS-PAGE and western blot. Protein signals were visualized using the
702 Odyssey DLx scanner (Li-Cor) and quantified using the Odyssey Empiria Studio program (Li-
703 Cor). Fluorescent signal from total protein staining (Li-Cor Total Protein Stain workflow) was
704 used to normalize signals for target proteins.
705
706 **SLAM-seq**
707 SLAM-seq was performed as previously described[34]. Briefly, following DMSO or IAA treatment,
708 *S. cerevisiae* cultures were treated with 5 mM 4-thiouracil (4tU) in DMSO or with DMSO alone
709 for 4 min. Cells were immediately fixed in cold methanol on dry ice and stored at –80°C. The
710 OD600 at the time of collection was ~0.7. *S. pombe* cultures were treated with 4tU and collected
711 using the same procedure. Three biological replicates were collected for all experiments. RNA
712 purification and DNase I treatment were performed using the Quick-RNA Fungal/Bacterial
713 Miniprep kit (Zymo Research) according to the manufacturer's recommendations under
714 reducing conditions, as described. Five micrograms of total RNA was used for alkylation. A total
715 of 200 ng of alkylated RNA was used to construct 3′ mRNA sequencing libraries. Libraries were
716 sequenced on a NovaSeq 6000 (Illumina) at the Oklahoma Medical Research Foundation
717 (OMRF) Clinical Genomics Center (Oklahoma City, OK, USA).
718
719 **SLAM-seq data analysis**
720 Data (paired-end 150 bp reads) were analyzed as previously described[34]. Preprocessing and
721 processing steps were implemented as a Snakemake workflow
722 (https://github.com/DonczewLab/SLAM-Seq_Analysis). Briefly, reads were preprocessed using
723 fastp (version 0.23.2)[53] and bbduk (BBMap version 39.06)
724 (https://sourceforge.net/projects/bbmap/). Reads were then aligned and processed using SLAM-

725 DUNK (version 0.4.3)[54]. Total read counts were defined as the number of reads remaining after
726 alignment and filtering in SLAM-DUNK. T>C read counts were defined as the number of reads
727 containing ≥2 T>C conversions. Genes with zero T>C read counts in one or more replicate
728 samples among all 25 min depletion experiments were excluded. Normalization and differential
729 expression analyses were performed on T>C read counts using DESeq2 (version 1.38.3)[55].
730 Normalization factors were calculated using total read counts for 25 min depletion experiments.
731 Because large changes in total read counts were expected after 3 h depletion, spike-in read
732 counts were used for normalization in those experiments. Genes that did not meet DESeq2
733 criteria for fold-change and/or *p*-value calculation were excluded from downstream analyses.
734

735 **ChEC-seq**

736 ChEC-seq was performed as previously described with minor modifications[2,56,57]. Briefly, 50 ml
737 *S. cerevisiae* cultures were pelleted at 2000 × g for 3 min. Cells were resuspended in 1 ml of
738 Buffer A (15 mM Tris-HCl [pH 7.5], 80 mM KCl, 0.1 mM EGTA, 0.2 mM spermine [Millipore
739 Sigma], 0.3 mM spermidine [Millipore Sigma], 1X protease inhibitors [2 µg/ml aprotinin, 1 µg/ml
740 pepstatin A, 1 µg/ml leupeptin, 2 mM PMSF]), transferred to a 1.5 ml microcentrifuge tube, and
741 pelleted at 1500 × g for 30 s. Cells were washed twice with 1 ml of Buffer A and resuspended in
742 570 µl of Buffer A. Thirty microliters of 2% digitonin (Millipore Sigma) was added to a final
743 concentration of 0.1%, and cells were permeabilized for 5 min at 30°C with shaking (900 rpm).
744 Samples were incubated with 0.2 mM CaCl2 for 5 min at 30°C with shaking. A 100 µl fraction of
745 the suspension was mixed with 100 µl of Stop Solution (400 mM NaCl, 20 mM EDTA, 4 mM
746 EGTA). Samples were then incubated with 0.4 mg/ml Proteinase K (Thermo Fisher Scientific)
747 for 30 min at 55°C. DNA was purified using the ChIP DNA Clean and Concentrator kit (Zymo
748 Research) and eluted in 30 µl of elution buffer. Samples were treated with 0.3 mg/ml RNase A
749 (Thermo Fisher Scientific) for 20 min at 37°C. Thirty microliters of Sera-Mag Speedbeads
750 (Cytiva), prepared as described (dx.doi.org/10.17504/protocols.io.x54v9p7b1g3e/v2), were
751 added, and samples were incubated for 10 min at room temperature. Supernatants were
752 transferred to a new tube, and the volume was adjusted to 175 µl (10 mM Tris-HCl, pH 8.0).
753 DNA was purified again using the ChIP DNA Clean and Concentrator kit and eluted in 30 µl of
754 Elution Buffer. Libraries were prepared using the Next Ultra II DNA Library Prep kit (New
755 England Biolabs) as described[58] and sequenced on a NovaSeq 6000 at the OMRF Clinical
756 Genomics Center.
757

758 **ChEC-seq data analysis**

759 Data (paired-end 150 bp reads) were analyzed as previously described with minor
760 modifications[2,56]. Initial preprocessing and processing steps were implemented as a Snakemake
761 workflow (https://github.com/DonczewLab/ChEC-Seq_Analysis). Briefly, reads were
762 preprocessed using bbduk (BBMap version 39.06) (https://sourceforge.net/projects/bbmap/) and
763 aligned using Bowtie 2 (version 2.5.0)[59]. BAM files were generated, sorted, and indexed using
764 Samtools (version 1.18)[60]. Genome coverage was calculated and normalized by counts per
765 million (CPM) using deepTools2 (version 3.5.4)[61]. Average genome coverage across replicates
766 was calculated using BEDTools (version 2.30.0)[62] and bedGraphToBigWig[63]. SAM files for *S.*
767 *cerevisiae* were converted to tag directories using the HOMER[64] 'makeTagDirectory' tool. Peaks
768 were called using the HOMER 'findPeaks' tool with optional arguments set to '-o auto -C 0 L 2 F
769 2', using the free MNase dataset as a control[2]. These settings apply a default false discovery
770 rate (FDR; 0.1%) and require peaks to be enriched twofold over the control and twofold over the
771 local background. Resulting peak files were converted to BED format using the 'pos2bed.pl'
772 program. For each peak, the summit was defined as the midpoint between the peak borders.
773 For promoter assignment, the list of annotated ORF sequences (excluding entries classified as
774 'dubious' or 'pseudogene') was downloaded from the SGD website
775 (https://www.yeastgenome.org). Data for 5888 genes were merged with TSS positions[65]. If TSS
776 annotation was missing, the TSS was manually assigned at −100 bp relative to the start codon.
777 At this stage, biological replicates were averaged for each sample. Peaks were assigned to
778 promoters if their summit was located between −300 and +100 bp relative to the TSS. When
779 more than one peak mapped to a promoter, the peak closest to the TSS was used. Promoters
780 bound in at least two out of four replicate experiments were included in the final list. To quantify
781 log2 changes in promoter occupancy, signal per promoter was calculated as the sum of
782 normalized reads within a 200 bp window centered on the promoter peak summit.
783

784 **ET-interacting motif discovery**

785 Putative ET-interacting motifs (ETMs) were identified using SLiMSearch (version 4) [66]. The
786 previously described ETMs Φ[+]Φ[+] and (Φ/[+])ΦΦ[+](Φ/[+]), where Φ is M, L, V, I, or F and [+]
787 is K or R[17], were used as input to query the *S. cerevisiae* proteome. ETMs were limited to those
788 present in nuclear proteins based on evidence in AllianceMine[67]. Overlapping and/or adjacent
789 ETMs were collapsed. Disorder propensity and accessibility were calculated in SLiMSearch
790 using IUPred2A[68] and AlphaFold RSA[69], respectively.
791

792 **Structural predictions**

793 Initial folding experiments involving characterized BRD4-interacting peptides and the BRD4 ET
794 domain or the Bdf1 ET domain were performed using a locally installed instance of AlphaFold2
795 (version 2.3.2)[37,70]. Experimental structures were obtained from the Protein Data Bank (PDB)[71].
796 ChimeraX (version 1.10.1)[72] was used to visualize structures and calculate structural similarity
797 and interfacial contacts. Similarity between experimental and predicted structures was
798 calculated as root mean square deviation (RMSD). Contacts were calculated as the number of
799 interfacial residue pairs ≤ 4.0 Å apart with a maximum predicted aligned error (PAE) ≤ 5.0 Å.
800 ETMs in nuclear proteins (*n* = 2418) were folded with the Bdf1 ET domain using two
801 implementations of AlphaFold2 : the locally installed AlphaFold2 instance (as above) and
802 ColabFold Batch (version 1.5.5)[73] run on Google Colaboratory. Eight amino acids N-terminal
803 and eight amino acids C-terminal to each ETM were included in folding experiments.
804 Confidence metrics were calculated using the ipSAE program (version 3)[74]. Cutoffs of PAE ≤ 10
805 Å and distance ≤ 10 Å were used to compute ipSAE scores. Combined ipSAE confidence was
806 calculated as the unweighted z-score average (scaled 0-1) across ipSAE scores of the top-
807 ranked AlphaFold2 and ColabFold models. Combined pDockQ2 confidence was calculated as
808 the unweighted z-score average (scaled 0-1) across pDockQ2 scores of the top-ranked
809 AlphaFold2 and ColabFold models. The DSSP program (version 4.5.6)[75] was used to assign
810 secondary structure elements (i.e., interfacial β-sheet establishment) in predicted structures.
811 FoldScore was calculated based on conditional interfacial β-sheet establishment across top-
812 ranked AlphaFold2 and ColabFold models: a FoldScore of 1 indicates that interfacial β-sheets
813 with the same orientation were assigned in both models; a FoldScore of 0.5 indicates that
814 interfacial β-sheets with different orientations were assigned in the two models or that an
815 interfacial β-sheet was assigned in only one model; and a FoldScore of 0 indicates that an
816 interfacial β-sheet was not assigned in either model.
817
818 **Chromatin mass spectrometry**
819 Chromatin-enriched fractions and whole cell extract were collected using chromatin-enriched
820 fractionation (ChEF) as previously described, with modifications[76]. Briefly, *S. cerevisiae* was
821 grown in 200 ml YPD medium at 30°C with shaking at 220 rpm to an OD600 of ~0.5 and split
822 into two 100 ml cultures. Cultures were treated with IAA or DMSO for 25 min. Cells were
823 pelleted at 2000 × g for 3 min, washed once with sterile water, and stored at –80°C. The OD600
824 at the time of collection was ~0.7. A minimum of five biological replicates were collected. Cells
825 were resuspended in 1 ml ChEF buffer 1 [76] supplemented with 1X phosphatase inhibitors (Apex
826 Biotechnology), 1X deacetylase inhibitors (Apex Biotechnology), and 1X protease inhibitors (see

827 above). Cells were combined with 1.5 ml disruption beads and processed in a Mini-Beadbeater-
828 24 (Biospec Products) at 3800 rpm for 30 s followed by incubation on ice for 2 min, repeated 10
829 times. Cell lysate was recovered as previously described[77] and cleared twice by centrifugation
830 at 500 × g for 5 min at 4°C. A fraction of the cleared lysate represented whole cell extract. The
831 remaining lysate was processed as described previously[76], except that ChEF buffer 2 was
832 supplemented with 1X phosphatase inhibitors, 1X deacetylase inhibitors, and 1X protease
833 inhibitors. Chromatin-enriched fractions were resuspended in 50 mM Tris-HCl (pH 7.5).
834
835 A total of 15 pmoles of bovine serum albumin (BSA) was added to 100 µg of total protein from
836 chromatin-enriched fractions or 200 µg of total protein from whole cell extracts as an internal
837 standard. Samples were processed as previously described[78]. Samples from chromatin-
838 enriched fractions were analyzed using a Q Exactive Plus mass spectrometer system
839 (ThermoFisher Scientific) in data-independent acquisition (DIA) mode with a 20 m/z window.
840 Samples from whole cell extracts were analyzed using an Exploris 480 mass spectrometer
841 system (ThermoFisher Scientific) in DIA mode with a 10 m/z window. Data were analyzed using
842 DIA-NN (version 1.9.2)[79] searching against the *S. cerevisiae* UniProt protein database
843 (downloaded from ENA/EMBL, accession GCA_000146045.2).
844
845 **Parallel reaction monitoring mass spectrometry**
846 Whole cell extracts and chromatin-enriched fractions were collected as described above. A total
847 of 14 pmoles of BSA was added to 60 µg of total protein from chromatin-enriched fractions or
848 100 µg of total protein from whole cell extracts as an internal standard. Samples were
849 processed as previously described[78] and analyzed using a Stellar mass spectrometer system
850 (ThermoFisher Scientific) in PRM mode with a resolution of 1.2 Da and a scan rate of 67
851 kDa/sec. Data were processed using Skyline (version 25.1)[80] to identify and integrate
852 chromatographic peaks for a defined set of validated peptides. Retention times were calibrated
853 using BSA and trypsin peptides. Protein abundance was calculated as the geometric mean of a
854 minimum of two monitored peptides normalized to the BSA internal standard and expressed as
855 pmol per 10 µg of total protein.
856
857 **Yeast two-hybrid analysis**
858 Yeast two-hybrid experiments were performed using the Matchmaker Gold Y2H system (Takara
859 Bio) based on the manufacturer's recommendations with modifications. Briefly, the *S. cerevisiae*
860 strain Y2HGold was co-transformed with *TRP1*-marked Gal4-BD and *LEU2*-marked Gal4-AD

plasmids, pGBKT7 and pGADT7, respectively. Co-transformed strains were cultured in SC-Leu-Trp medium at 30°C overnight, adjusted to an OD600 of 1, and serially diluted tenfold. Five microliters of each dilution was spotted onto SC-Leu-Trp, SC-Leu-Trp-His, or SC-Leu-Trp-His plates supplemented with 2 mM 3-Amino-1,2,4-triazole (3-AT, MilliporeSigma). Plates were incubated at 30°C and imaged daily for a minimum of four days.

Acknowledgments

We thank Linda Thompson, Dean Dawson, Christopher Sansam and Karen Arndt for helpful comments, Steven Hahn for plasmids, and Stephen Buratowski for anti-Bdf1 antibody. We thank the OMRF Research Computing Services, Clinical Genomics Center, and Center for Biomedical Data Sciences for contributions to this work.

Funding

National Science Foundation grant 2346844 (RD).
National Institutes of Health grant R35GM160259 (RD).
National Institutes of Health grant P20GM103636 (Project 2, RD).
Oklahoma Center for Adult Stem Cell Research grant 231012 (RD).
National Institutes of Health grant P30GM149376 (Bioinformatics and Pathway Core, KB).

Author contributions

Conceptualization: JR, MD, RD
Methodology: JR, MD, MK, KB, RD
Investigation: IP, JR, AM, MD, MK, RD
Visualization: IP, JR, AM, RD
Supervision: JR, MD, RD
Writing—original draft: RD
Writing—review & editing: JR, MD, RD

Competing interests

The authors declare no competing interests.

Data and materials availability

All data are available in the main text or the supplementary materials. SLAM-seq and ChEC-seq datasets have been deposited in the NCBI Gene Expression Omnibus (GEO) under accession

895 number GSE313013. Raw datasets from DIA and PRM mass spectrometry experiments have
896 been deposited in the Zenodo repository (https://doi.org/10.5281/zenodo.17966389). Reference
897 genome assemblies and annotations for *S. cerevisiae* strain S288C (version R64-3-1) and *S.*
898 *pombe* strain 972h- (version ASM294v2) were retrieved from the NCBI Datasets repository
899 (GCF 000146045.2 and GCF 000002945.1, respectively). BED files for *S. cerevisiae* and *S.*
900 *pombe* used in SLAM-DUNK were retrieved from the Zenodo repository
901 (https://doi.org/10.5281/zenodo.10714018).
902
903 **References**

904 1. Filippakopoulos, P. *et al.* Histone Recognition and Large-Scale Structural Analysis of the
905 Human Bromodomain Family. *Cell* **149**, 214–231 (2012).
906 2. Donczew, R. & Hahn, S. BET family members Bdf1/2 modulate global transcription initiation
907 and elongation in Saccharomyces cerevisiae. *Elife* **10**, e69619 (2021).
908 3. Muhar, M. *et al.* SLAM-seq defines direct gene-regulatory functions of the BRD4-MYC axis.
909 *Science* **360**, 800–805 (2018).
910 4. Winter, G. E. *et al.* BET Bromodomain Proteins Function as Master Transcription Elongation
911 Factors Independent of CDK9 Recruitment. *Molecular Cell* **67**, 5-18.e19 (2017).
912 5. Zheng, B. *et al.* Distinct layers of BRD4-PTEFb reveal bromodomain-independent function
913 in transcriptional regulation. *Molecular Cell* **83**, 2896-2910.e4 (2023).
914 6. Fujisawa, T. & Filippakopoulos, P. Functions of bromodomain-containing proteins and their
915 roles in homeostasis and cancer. *Nature Reviews Molecular Cell Biology* **18**, 246–262
916 (2017).
917 7. Wang, N., Wu, R., Tang, D. & Kang, R. The BET family in immunity and disease. *Signal*
918 *Transduction and Targeted Therapy* **6**, 1–22 (2021).
919 8. Filippakopoulos, P. *et al.* Selective inhibition of BET bromodomains. *Nature* **468**, 1067–1073
920 (2010).
921 9. Nicodeme, E. *et al.* Suppression of inflammation by a synthetic histone mimic. *Nature* **468**,
922 1119–1123 (2010).

923 10. Shu, S. *et al.* Response and resistance to BET bromodomain inhibitors in triple-negative
924 breast cancer. *Nature* **529**, 413–417 (2016).
925 11. Calder, J., Nagelberg, A., Luu, J., Lu, D. & Lockwood, W. W. Resistance to BET inhibitors in
926 lung adenocarcinoma is mediated by casein kinase phosphorylation of BRD4. *Oncogenesis*
927 **10**, 27 (2021).
928 12. Sun, Y. *et al.* Epigenetic heterogeneity promotes acquired resistance to BET bromodomain
929 inhibition in ovarian cancer. *Am J Cancer Res* **11**, 3021–3038 (2021).
930 13. Arnold, M., Bressin, A., Jasnovidova, O., Meierhofer, D. & Mayer, A. A BRD4-mediated
931 elongation control point primes transcribing RNA polymerase II for 3'-processing and
932 termination. *Mol Cell* S1097-2765(21)00506–2 (2021) doi:10.1016/j.molcel.2021.06.026.
933 14. Zheng, B. *et al.* BRD2 bridges TFIID and MOF-H4K16ac-containing nucleosomes to
934 promote transcriptional initiation. *Molecular Cell* https://doi.org/10.1016/j.molcel.2025.12.010
935 (2025) doi:10.1016/j.molcel.2025.12.010.
936 15. Matangkasombut, O., Buratowski, R. M., Swilling, N. W. & Buratowski, S. Bromodomain
937 factor 1 corresponds to a missing piece of yeast TFIID. *Genes Dev.* **14**, 951–962 (2000).
938 16. Kanno, T. *et al.* BRD4 assists elongation of both coding and enhancer RNAs by interacting
939 with acetylated histones. *Nat Struct Mol Biol* **21**, 1047–1057 (2014).
940 17. Lambert, J.-P. *et al.* Interactome Rewiring Following Pharmacological Targeting of BET
941 Bromodomains. *Mol Cell* **73**, 621-638.e17 (2019).
942 18. Matangkasombut, O. & Buratowski, S. Different sensitivities of bromodomain factors 1 and 2
943 to histone H4 acetylation. *Mol. Cell* **11**, 353–363 (2003).
944 19. Slaughter, M. J. *et al.* HDAC inhibition results in widespread alteration of the histone
945 acetylation landscape and BRD4 targeting to gene bodies. *Cell Rep* **34**, 108638 (2021).
946 20. Kayne, P. S. *et al.* Extremely conserved histone H4 N terminus is dispensable for growth but
947 essential for repressing the silent mating loci in yeast. *Cell* **55**, 27–39 (1988).

948 21. Ranish, J. A. *et al.* The study of macromolecular complexes by quantitative proteomics. *Nat.*
949 *Genet.* **33**, 349–355 (2003).
950 22. Zhang, S. & Roeder, R. G. Resistance of estrogen receptor function to BET bromodomain
951 inhibition is mediated by transcriptional coactivator cooperativity. *Nat Struct Mol Biol* 1–15
952 (2024) doi:10.1038/s41594-024-01384-6.
953 23. Rahman, S. *et al.* The Brd4 extraterminal domain confers transcription activation
954 independent of pTEFb by recruiting multiple proteins, including NSD3. *Mol Cell Biol* **31**,
955 2641–2652 (2011).
956 24. Zhang, Q. *et al.* Structural Mechanism of Transcriptional Regulator NSD3 Recognition by
957 the ET Domain of BRD4. *Structure* **24**, 1201–1208 (2016).
958 25. Konuma, T. *et al.* Structural Mechanism of the Oxygenase JMJD6 Recognition by the
959 Extraterminal (ET) Domain of BRD4. *Sci Rep* **7**, 16272 (2017).
960 26. Alerasool, N., Leng, H., Lin, Z.-Y., Gingras, A.-C. & Taipale, M. Identification and functional
961 characterization of transcriptional activators in human cells. *Molecular Cell* **82**, 677-695.e7
962 (2022).
963 27. Trojanowski, J. *et al.* Transcription activation is enhanced by multivalent interactions
964 independent of phase separation. *Molecular Cell* **82**, 1878-1893.e10 (2022).
965 28. Xing, E. *et al.* Development of Murine Leukemia Virus Integrase-Derived Peptides That Bind
966 Brd4 Extra-Terminal Domain as Candidates for Suppression of Acute Myeloid Leukemia.
967 *ACS Pharmacol. Transl. Sci.* **4**, 1628–1638 (2021).
968 29. Huang, Q. *et al.* Peptide Inhibitor Targeting the Extraterminal Domain in BRD4 Potently
969 Suppresses Breast Cancer Both In Vitro and In Vivo. *J. Med. Chem.* **67**, 6658–6672 (2024).
970 30. Wu, S.-Y., Lee, A.-Y., Lai, H.-T., Zhang, H. & Chiang, C.-M. Phospho switch triggers Brd4
971 chromatin binding and activator recruitment for gene-specific targeting. *Mol Cell* **49**, 843–
972 857 (2013).

973 31. Malvezzi, F. *et al.* Phosphorylation-dependent BRD4 dimerization and implications for
974 therapeutic inhibition of BET family proteins. *Commun Biol* **4**, 1–13 (2021).
975 32. Sawa, C. *et al.* Bromodomain factor 1 (Bdf1) is phosphorylated by protein kinase CK2. *Mol.*
976 *Cell. Biol.* **24**, 4734–4742 (2004).
977 33. Han, X. *et al.* Roles of the BRD4 short isoform in phase separation and active gene
978 transcription. *Nat Struct Mol Biol* **27**, 333–341 (2020).
979 34. Ridenour, J. B. & Donczew, R. An end-to-end workflow to study newly synthesized mRNA
980 following rapid protein depletion in Saccharomyces cerevisiae. *BMC Methods* **1**, 8 (2024).
981 35. Donczew, R., Warfield, L., Pacheco, D., Erijman, A. & Hahn, S. Two roles for the yeast
982 transcription coactivator SAGA and a set of genes redundantly regulated by TFIID and
983 SAGA. *eLife* **9**, e50109 (2020).
984 36. Zentner, G. E., Kasinathan, S., Xin, B., Rohs, R. & Henikoff, S. ChEC-seq kinetics
985 discriminates transcription factor binding sites by DNA sequence and shape in vivo. *Nature*
986 *Communications* **6**, 8733 (2015).
987 37. Jumper, J. *et al.* Highly accurate protein structure prediction with AlphaFold. *Nature* **596**,
988 583–589 (2021).
989 38. Zhou, D. *et al.* FACT subunit SUPT16H associates with BRD4 and contributes to silencing
990 of interferon signaling. *Nucleic Acids Res* **50**, 8700–8718 (2022).
991 39. Peterson, A. C., Russell, J. D., Bailey, D. J., Westphall, M. S. & Coon, J. J. Parallel Reaction
992 Monitoring for High Resolution and High Mass Accuracy Quantitative, Targeted Proteomics
993 *. *Molecular & Cellular Proteomics* **11**, 1475–1488 (2012).
994 40. True, J. D. *et al.* The Modifier of Transcription 1 (Mot1) ATPase and Spt16 Histone
995 Chaperone Co-regulate Transcription through Preinitiation Complex Assembly and
996 Nucleosome Organization*. *Journal of Biological Chemistry* **291**, 15307–15319 (2016).
997 41. Viktorovskaya, O. *et al.* Essential histone chaperones collaborate to regulate transcription
998 and chromatin integrity. *Genes Dev.* **35**, 698–712 (2021).

42. Connell, Z., Parnell, T. J., McCullough, L. L., Hill, C. P. & Formosa, T. The interaction between the Spt6-tSH2 domain and Rpb1 affects multiple functions of RNA Polymerase II. *Nucleic Acids Res* **50**, 784–802 (2022).
43. Garcia-Gutierrez, P., Mundi, M. & Garcia-Dominguez, M. Association of bromodomain BET proteins with chromatin requires dimerization through the conserved motif B. *Journal of Cell Science* **125**, 3671–3680 (2012).
44. Stortz, M., Presman, D. M. & Levi, V. Transcriptional condensates: a blessing or a curse for gene regulation? *Commun Biol* **7**, 1–10 (2024).
45. Sabari, B. R. *et al.* Coactivator condensation at super-enhancers links phase separation and gene control. *Science* **361**, (2018).
46. Gilan, O. *et al.* Selective targeting of BD1 and BD2 of the BET proteins in cancer and immunoinflammation. *Science* **368**, 387–394 (2020).
47. Christiano, R., Nagaraj, N., Fröhlich, F. & Walther, T. C. Global Proteome Turnover Analyses of the Yeasts *S. cerevisiae* and *S. pombe*. *Cell Reports* **9**, 1959–1965 (2014).
48. Mahendrawada, L., Warfield, L., Donczew, R. & Hahn, S. Low overlap of transcription factor DNA binding and regulatory targets. *Nature* **642**, 796–804 (2025).
49. Roy, K. & Chanfreau, G. Stress-Induced Nuclear RNA Degradation Pathways Regulate Yeast Bromodomain Factor 2 to Promote Cell Survival. *PLOS Genetics* **10**, e1004661 (2014).
50. Brachmann, C. B. *et al.* Designer deletion strains derived from Saccharomyces cerevisiae S288C: a useful set of strains and plasmids for PCR-mediated gene disruption and other applications. *Yeast* **14**, 115–132 (1998).
51. Warfield, L. *et al.* Transcription of Nearly All Yeast RNA Polymerase II-Transcribed Genes Is Dependent on Transcription Factor TFIID. *Mol Cell* **68**, 118-129.e5 (2017).
52. Sikorski, R. S. & Hieter, P. A system of shuttle vectors and yeast host strains designed for efficient manipulation of DNA in Saccharomyces cerevisiae. *Genetics* **122**, 19–27 (1989).

1025 53. Chen, S., Zhou, Y., Chen, Y. & Gu, J. fastp: an ultra-fast all-in-one FASTQ preprocessor.
1026 *Bioinformatics* **34**, i884–i890 (2018).
1027 54. Neumann, T. *et al.* Quantification of experimentally induced nucleotide conversions in high-
1028 throughput sequencing datasets. *BMC Bioinformatics* **20**, 258 (2019).
1029 55. Love, M. I., Huber, W. & Anders, S. Moderated estimation of fold change and dispersion for
1030 RNA-seq data with DESeq2. *Genome Biology* **15**, 550 (2014).
1031 56. Mahendrawada, L., Warfield, L., Donczew, R. & Hahn, S. Low overlap of transcription factor
1032 DNA binding and regulatory targets. *Nature* 1–9 (2025) doi:10.1038/s41586-025-08916-0.
1033 57. Warfield, L., Donczew, R., Mahendrawada, L. & Hahn, S. Yeast Mediator facilitates
1034 transcription initiation at most promoters via a Tail-independent mechanism. *Molecular Cell*
1035 **82**, 4033-4048.e7 (2022).
1036 58. Möller, M., Ridenour, J. B., Wright, D. F., Martin, F. A. & Freitag, M. H4K20me3 is important
1037 for Ash1-mediated H3K36me3 and transcriptional silencing in facultative heterochromatin in
1038 a fungal pathogen. *PLOS Genetics* **19**, e1010945 (2023).
1039 59. Langmead, B. & Salzberg, S. L. Fast gapped-read alignment with Bowtie 2. *Nature Methods*
1040 **9**, 357–359 (2012).
1041 60. Danecek, P. *et al.* Twelve years of SAMtools and BCFtools. *Gigascience* **10**, giab008
1042 (2021).
1043 61. Ramírez, F. *et al.* deepTools2: a next generation web server for deep-sequencing data
1044 analysis. *Nucleic Acids Research* **44**, W160–W165 (2016).
1045 62. Quinlan, A. R. & Hall, I. M. BEDTools: a flexible suite of utilities for comparing genomic
1046 features. *Bioinformatics* **26**, 841–842 (2010).
1047 63. Kent, W. J., Zweig, A. S., Barber, G., Hinrichs, A. S. & Karolchik, D. BigWig and BigBed:
1048 enabling browsing of large distributed datasets. *Bioinformatics* **26**, 2204–2207 (2010).

1049 64. Heinz, S. *et al.* Simple combinations of lineage-determining transcription factors prime cis-
1050 regulatory elements required for macrophage and B cell identities. *Mol Cell* **38**, 576–589
1051 (2010).
1052 65. Park, D., Morris, A. R., Battenhouse, A. & Iyer, V. R. Simultaneous mapping of transcript
1053 ends at single-nucleotide resolution and identification of widespread promoter-associated
1054 non-coding RNA governed by TATA elements. *Nucleic Acids Res* **42**, 3736–3749 (2014).
1055 66. Krystkowiak, I. & Davey, N. E. SLiMSearch: a framework for proteome-wide discovery and
1056 annotation of functional modules in intrinsically disordered regions. *Nucleic Acids Research*
1057 **45**, W464–W469 (2017).
1058 67. The Alliance of Genome Resources Consortium. Updates to the Alliance of Genome
1059 Resources central infrastructure. *Genetics* **227**, iyae049 (2024).
1060 68. Mészáros, B., Erdős, G. & Dosztányi, Z. IUPred2A: context-dependent prediction of protein
1061 disorder as a function of redox state and protein binding. *Nucleic Acids Res* **46**, W329–
1062 W337 (2018).
1063 69. Piovesan, D., Monzon, A. M. & Tosatto, S. C. E. Intrinsic protein disorder and conditional
1064 folding in AlphaFoldDB. *Protein Science* **31**, e4466 (2022).
1065 70. Evans, R. *et al.* Protein complex prediction with AlphaFold-Multimer. 2021.10.04.463034
1066 Preprint at https://doi.org/10.1101/2021.10.04.463034 (2022).
1067 71. Berman, H. M. *et al.* The Protein Data Bank. *Nucleic Acids Res* **28**, 235–242 (2000).
1068 72. Meng, E. C. *et al.* UCSF ChimeraX: Tools for structure building and analysis. *Protein*
1069 *Science* **32**, e4792 (2023).
1070 73. Mirdita, M. *et al.* ColabFold: making protein folding accessible to all. *Nat Methods* **19**, 679–
1071 682 (2022).
1072 74. Dunbrack, R. L. Rēs ipSAE loquunt: What's wrong with AlphaFold's ipTM score and how to
1073 fix it. 2025.02.10.637595 Preprint at https://doi.org/10.1101/2025.02.10.637595 (2025).

1074 75. Hekkelman, M. L., Salmoral, D. Á., Perrakis, A. & Joosten, R. P. DSSP 4: FAIR annotation
1075 of protein secondary structure. *Protein Science* **34**, e70208 (2025).
1076 76. Cuevas-Bermúdez, A., Garrido-Godino, A. I. & Navarro, F. A novel yeast chromatin-
1077 enriched fractions purification approach, yChEFs, for the chromatin-associated protein
1078 analysis used for chromatin-associated and RNA-dependent chromatin-associated
1079 proteome studies from *Saccharomyces cerevisiae*. *Gene Reports* **16**, 100450 (2019).
1080 77. de Jonge, W. J., Brok, M., Kemmeren, P. & Holstege, F. C. P. An Optimized Chromatin
1081 Immunoprecipitation Protocol for Quantification of Protein-DNA Interactions. *STAR*
1082 *Protocols* **1**, 100020 (2020).
1083 78. Rindler, P. M., Plafker, S. M., Szweda, L. I. & Kinter, M. High Dietary Fat Selectively
1084 Increases Catalase Expression within Cardiac Mitochondria *. *Journal of Biological*
1085 *Chemistry* **288**, 1979–1990 (2013).
1086 79. Demichev, V., Messner, C. B., Vernardis, S. I., Lilley, K. S. & Ralser, M. DIA-NN: neural
1087 networks and interference correction enable deep proteome coverage in high throughput.
1088 *Nat Methods* **17**, 41–44 (2020).
1089 80. Pino, L. K. *et al.* The Skyline ecosystem: Informatics for quantitative mass spectrometry
1090 proteomics. *Mass Spectrometry Reviews* **39**, 229–244 (2020).
1091 81. Lin, Y.-J. *et al.* Solution structure of the extraterminal domain of the bromodomain-
1092 containing protein BRD4. *Protein Science* **17**, 2174–2179 (2008).
1093 82. Wang, Y. *et al.* Coiled-coil networking shapes cell molecular machinery. *MBoC* **23**, 3911–
1094 3922 (2012).
1095
1096
1097